

AD-A094 085

PURDUE UNIV LAFAYETTE IND SCHOOL OF AERONAUTICS AND --ETC F/G 12/1
USE OF STRAINED COORDINATE PERTURBATION METHOD IN TRANSONIC AER--ETC(U)
OCT 80 P GURUSWAMY AFOSR-78-3523

UNCLASSIFIED

AFWAL-TR-80-3102

NL

END

DATE

FILMED

2, 804

DTİÇ

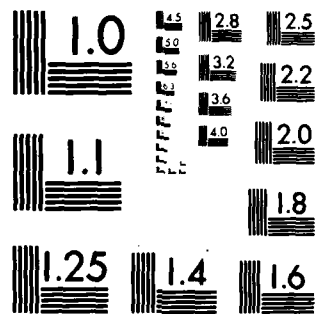
END

DATA

FILMED

2. 5

DTIC



MICROCOPY RESOLUTION TEST CHART
NATIONAL BUREAU OF STANDARDS-1963-A

AFWAL-TR-80-3102

AD A094085

USE OF STRAINED COORDINATE PERTURBATION METHOD IN TRANSONIC
AEROELASTIC COMPUTATIONS

P. GURUSWAMY
PURDUE UNIVERSITY
WEST LAFAYETTE, INDIANA 47907

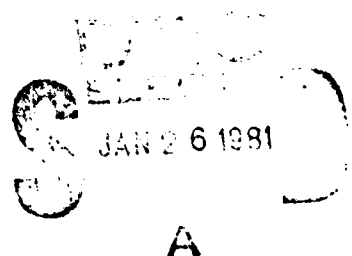
OCTOBER 1980



TECHNICAL REPORT AFWAL-TR-80-3102
Final Report for period November 1979-June 1980

Approved for public release; distribution unlimited.

FLIGHT DYNAMICS LABORATORY
AIR FORCE WRIGHT AERONAUTICAL LABORATORIES
AIR FORCE SYSTEMS COMMAND
WRIGHT-PATTERSON AIR FORCE BASE, OHIO 45433



DOC FILE COPY

81 1 23 076

NOTICE

When Government drawings, specifications, or other data are used for any purpose other than in connection with a definitely related Government procurement operation, the United States Government thereby incurs no responsibility nor any obligation whatsoever; and the fact that the government may have formulated, furnished, or in any way supplied the said drawings, specifications, or other data, is not to be regarded by implication or otherwise as in any manner licensing the holder or any other person or corporation, or conveying any rights or permission to manufacture, use, or sell any patented invention that may in any way be related thereto.


This report has been reviewed by the Office of Public Affairs (PA) and is releasable to the general public, including foreign nations.

This technical report has been reviewed and is approved for publication.


LAWRENCE J. HUTTSELL
Aerospace Engineer
Aeroelastic Group


FREDERICK A. PICCHIONI, Lt Col, USAF
Ch, Analysis and Optimization Branch

FOR THE COMMANDER


RALPH L. KUSTER, Jr, Col, USAF
Chief, Structures and Dynamics Division

Copies of this report should not be returned unless return is required by security considerations, contractual obligations, or notice on a specific document.

(16) 2307 (17) N5

SECURITY CLASSIFICATION OF THIS PAGE (When Data Entered)

19 REPORT DOCUMENTATION PAGE		READ INSTRUCTIONS BEFORE COMPLETING FORM
1. REPORT NUMBER	2. GOVT ACCESSION NO.	3. RECIPIENT'S CATALOG NUMBER
18 AFWAL-TR-80-3102	AD-A094085	
4. TITLE (and Subtitle)		5. TYPE OF REPORT & PERIOD COVERED
6 USE OF STRAINED COORDINATE PERTURBATION METHOD IN TRANSONIC AEROELASTIC COMPUTATIONS.		Final Report. 3m November 1979-October 1980
7. AUTHOR(s)		8. CONTRACT OR GRANT NUMBER(s)
10 P. Guruswamy	15	AFOSR-78-35238
9. PERFORMING ORGANIZATION NAME AND ADDRESS		10. PROGRAM ELEMENT, PROJECT, TASK AREA & WORK UNIT NUMBERS
School of Aeronautics and Astronautics Purdue University West Lafayette, Indiana 47907		PE 61102F 2307/N5/11
11. CONTROLLING OFFICE NAME AND ADDRESS		12. REPORT DATE
Flight Dynamics Laboratories (FIBR) Air Force Wright Aeronautical Laboratories Wright-Patterson AFB, Ohio 45433		11 October 1980
14. MONITORING AGENCY NAME & ADDRESS (if different from Controlling Office)		13. NUMBER OF PAGES
12 47		46
16. DISTRIBUTION STATEMENT (of this Report)		15. SECURITY CLASS. (of this report)
Approved for public release; distribution unlimited		Unclassified
17. DISTRIBUTION STATEMENT (of the abstract entered in Block 20, if different from Report)		15a. DECLASSIFICATION/DOWNGRADING SCHEDULE
18. SUPPLEMENTARY NOTES		
19. KEY WORDS (Continue on reverse side if necessary and identify by block number)		
Perturbation Method Strained Coordinates Transonic Unsteady Aerodynamics Divergence Speed		
20. ABSTRACT (Continue on reverse side if necessary and identify by block number)		
The application of the strained coordinate perturbation method in transonic aeroelastic computations is investigated. The main objective is to reduce the computational time required for transonic aeroelastic calculations. Based on the strained coordinate perturbation equations, a procedure is presented to generate steady state initial conditions for LTRAN2 transonic code. Influence of such initial conditions on unsteady computations is studied. Results are illustrated for Mach number, angle of attack and thickness		

DD FORM 1 JAN 73 1473 EDITION OF 1 NOV 65 IS OBSOLETE

SECURITY CLASSIFICATION OF THIS PAGE (When Data Entered)

291850

✓
SECURITY CLASSIFICATION OF THIS PAGE(When Data Entered)

variations. The computer time required by the present procedure and the direct LTRAN2 computations are compared. There is a considerable saving in the computer time by present procedure.

The application of the strained coordinate perturbation method in computing transonic divergence speeds of a slender straight wing is presented. Results are obtained for a 10% thick parabolic arc at varying Mach number. Transonic divergence speeds obtained by present method are compared with those given by subsonic theory.

A computer program for creating the steady state initial conditions based on the strained coordinate perturbation method is presented. This program is compatible with LTRAN2.

✓

SECURITY CLASSIFICATION OF THIS PAGE(When Data Entered)

FOREWORD

This report was prepared by P. Guruswamy of the School of Aeronautics and Astronautics of Purdue University under AFOSR Grant 78-3523A, "Application of Time-Accurate Transonic Aerodynamics to Aeroelastic Problems". The report covers work conducted from November 1979 to June 1980. The research was administered by Lawrence J. Huttshell (AFWAL/FIBRC) of the Structures and Dynamics Division, Flight Dynamics Laboratory, Wright-Patterson Air Force Base, Ohio. The advice of Professor T. Y. Yang of Purdue University and Dr. J. Olsen of the Flight Dynamics Laboratory is also appreciated.

[illegible]

TABLE OF CONTENTS

SECTION	PAGE
I INTRODUCTION.	1
II STRAINED COORDINATE PERTURBATION EQUATIONS.	8
III APPLICATION TO STEADY AND UNSTEADY COMPUTATIONS	12
(a) Mach Number Variation.	12
(b) Angle of Attack Variation.	16
(c) Thickness Variation.	18
IV APPLICATION TO THE TRANSONIC DIVERGENCE PROBLEM.	22
(a) Formulation of Divergence Equations.	22
(b) Results.	25
V CONCLUDING REMARKS.	32
REFERENCES.	33
APPENDIX.	35

LIST OF ILLUSTRATIONS

FIGURE	PAGE
1 Effect of Mach Number Perturbation for 6% Thick Parabolic Arc on Steady Pressure Curves at $M = 0.86$	14
2 Effect of Mach Number Perturbation for 6% Thick Parabolic Arc on Unsteady Pressure Curves at $M = 0.86$	15
3 Effect of Angle of Attack Perturbation for 6% Thick Parabolic Arc on Steady Pressure Curves at $\alpha = 0.8^\circ$	17
4 Effect of Thickness Perturbation for 6.5% Thick Parabolic Arc on Steady Pressure Curves at $M = 0.85$ and $\alpha = 0.0^\circ$	19
5 Effect of Thickness Perturbation for 6.5% Thick Parabolic Arc on Unsteady Pressure Curves at $M = 0.85$ and $\alpha = 0.0^\circ$	21
6 Variation of Lift Coefficient with Angle of Attack for 10% Thick Parabolic Arc at $M = 0.80$	26
7 Variation of Moment (About Leading Edge) Coefficient with Angle of Attack for 10% Thick Parabolic Arc at $M = 0.80$	27
8 Effect of Mach Number on Static Divergence Dynamic Pressure for a Straight Slender Wing at Various Positions of Elastic Axis.	30

LIST OF TABLES

TABLE	PAGE
1 Aerodynamic Coefficients for 10% Thick Parabolic Arc at Various Mach Numbers.	29

NOMENCLATURE

a_h	distance between midchord and elastic axis in semichords, positive toward the trailing edge
c	full chord length of airfoil
C_L	lift coefficient
C_m	moment coefficient about leading edge
$C_{L\alpha}$	slope of the lift coefficient curve
$C_{m\alpha}$	slope of the moment coefficient curve
GJ	torsional rigidity of wing section
k_C	reduced frequency defined as $\omega c/U$
k	$(\gamma+1)M_\infty^2$, transonic flow parameter
M_∞	free stream Mach number
ρ	ratio of the semispan to chord
q	dynamic pressure defined as $1/2 \rho U^2$
U	free stream velocity
α	angle of attack
β	$1/(1-M_\infty^2)^{1/2}$, Prandtl-Glauert Number
γ	ratio of specific heats
δx_s	shock movement in chord per unit perturbation
ϵ	perturbation parameter
ρ	free stream air density
τ	ratio of the maximum airfoil thickness to chord
ϕ	disturbance velocity potential
ω	circular frequency of oscillation
(0)	denote parameters corresponding to base flow
(1)	denote parameters corresponding to calibration flow

SECTION I

INTRODUCTION

In recent years there is an increasing trend that aircraft be operated at a speed in high subsonic or transonic regimes. In transonic flight, small-amplitude oscillations of a wing can produce large variations in the aerodynamic forces and moments acting on that wing. Moreover, phase differences between the motion and the resulting forces and moments can be large. These characteristics tend to increase the probability of encountering aeroelastic instabilities. Thus, the transonic regime has become a sensitive one for aeroelastic analysis. Studies in transonic aeroelasticity have begun recently.

In References 1 to 5, Yang et al. have conducted various aeroelastic studies of airfoils in two dimensional transonic flows. In Reference 6, Eastep and Olsen have conducted the flutter analysis of a rectangular wing in three dimensional transonic flows. A state-of-the-art review on the aeroelastic applications of transonic aerodynamics is given by Ashley in Reference 7.

In transonic aeroelastic studies, the computation of aerodynamic forces is a major task. Previous transonic aeroelastic studies have shown that the computer time required to compute the aerodynamic data is quite high. It is due to the fact that the transonic aerodynamics depends on flow parameters such as Mach number, angle of attack, airfoil configuration, reduced frequency, etc. in a nonlinear fashion. Because of this, the aerodynamic computation has to be repeated whenever any one of the above flow parameters is varied. Also computations become more complicated when shocks are present.

The linear subsonic and supersonic aerodynamic equations yield closed form relations between aerodynamic forces and flow parameters. On the other hand, nonlinear transonic aerodynamic equations do not directly yield any such relations. Lack of such closed form relations has put restriction on certain transonic aeroelastic studies. For example, in order to compute the transonic divergence speed of a wing, it is required to know the aerodynamic forces as a function of angle of attack.

Recently some techniques based on perturbation method have been developed to avoid the repetition of the aerodynamic computation when flow parameters are varied. Such techniques have also led to simple relations between aerodynamic forces and flow parameters. One such technique is to use the concept of the strained coordinate perturbation procedure in obtaining the transonic aerodynamic loads.

The basic concept of the method of strained coordinate perturbation is to minimize the actual number of separate calculations required in a particular application by extending, over some parametric range, the usefulness of each individual solution determined by some computationally-expensive procedure. Coordinate straining introduced into transonic aerodynamics as a means of accounting properly for the movement of discontinuities (shock waves) due to changes in some geometric or flow parameter is shown to result in an accurate perturbation predictions in the vicinity of the discontinuity. Detailed studies of using this method as an effective tool for reducing the computational requirements in transonic aerodynamics has begun.

The basic concepts of coordinate straining is given, for example, in References 8 and 9. An evaluation of the strained coordinate perturbation procedure as applied to nonlinear subsonic and transonic flows is given by Stahara et al. in Reference 10.

In Reference 10, a procedure of defining a unit perturbation by employing two nonlinear solutions which differ from one another by a nominal change in some geometric or flow parameter, and then using that unit perturbation to predict a family of related nonlinear solutions over a range of parameter variation is discussed. Coordinate straining is used in determining the unit perturbation to account for movement of shocks due to the perturbation. Based on full potential solutions, perturbation results are presented for flows past both isolated airfoils and compressor cascades involving a variety of flow and geometry parameter changes in transonic regime. Comparisons with corresponding "exact" nonlinear solutions indicate a good accuracy and range of validity of such a method.

In Reference 11, Nixon illustrated a procedure of perturbing a transonic flow with shock wave. The method is based on the use of a distorted airfoil as the initial case rather than the real physical airfoil. The distortion is chosen such that the shock location is unchanged by the perturbation. The distorted airfoil is obtained by the use of a strained coordinate system. The procedure yielded an algebraic similarity relation between related airfoils with shock waves at different locations. Results are illustrated for a NACA 0012 airfoil and 10% thick parabolic arc at transonic Mach numbers. The pressure distributions around the perturbed airfoils computed by using both the extended integral equation method and the perturbation method compare well.

In Reference 12, Nixon extended the fundamental concept of Reference 11 to two-dimensional lifting flows and three-dimensional lifting flows with multiple, intersecting shock waves. The application of strained coordinate perturbation method in computing the steady transonic aerodynamic loads when Mach number and angle-of-attack are varied is illustrated. From this method, transonic steady-state aerodynamic solution at any given value of a parameter can be expressed as a function of the solutions obtained at two different values of the same parameter. The solutions required are termed as base and calibration solutions, respectively. The procedure is based on the assumptions that shocks are neither created nor destroyed within the range of variation of the parameter (Mach number or angle-of-attack) and the perturbation of the parameter is small. Using the method, simple algebraic expressions were derived for lift, pitching moment and drag coefficients in transonic regime. The method was illustrated for a 10% thick parabolic arc and a NACA 64A410 airfoil at transonic Mach numbers.

In Reference 13, Nixon compared the strained coordinate interpolation method used for transonic flow in Reference 12 with normal interpolation/extrapolation procedures. It was found that both methods are essentially equivalent in smooth regions of the solution. However, the normal linear extrapolation may not be applicable in the region just behind the shock wave. The strained coordinate method does move the shock and its associated shock foot singularity to the correct location and scales the strength of the singularity according to linear interpolation.

Based on the strained coordinate perturbation procedure the computational time required for transonic aeroelastic studies can considerably be reduced when parameters such as Mach number, angle-of-attack, thickness, etc. are varied. Using the developments, for example, in Reference 12, the repetition of steady state aerodynamic computations can be avoided when flow parameters are varied. Thus, there will be considerable reduction in the computational time for aeroelastic studies using the steady state computations. For example, in computing static divergence speed of a wing only steady state aerodynamic data is required.

Transonic unsteady computations based on time integration, indicial and harmonic methods require fairly accurate steady state initial conditions. It is noted that in both indicial and harmonic methods, the unsteady solution is treated as a small linear perturbation about a nonlinear steady state solution. When flow parameters are varied in unsteady computations, the required steady state initial conditions can be economically obtained by using the strained coordinate perturbation method.

Certain aeroelastic computations require the aerodynamic forces as a function of flow parameters. For example, in computing static divergence speed of a wing, it is necessary to know the aerodynamic forces as a function of angle-of-attack. Such functions for transonic regime can be obtained by the strained coordinate perturbation method.

In this study, some preliminary applications of the strained coordinate perturbation procedure in transonic aeroelasticity are investigated. The main emphasis is on reducing the computational time in transonic aeroelastic

studies. The developments in Reference 12 are used for this purpose.

First, the use of the strained coordinate perturbation method in computing the steady and unsteady aerodynamic pressure distributions for varying flow parameters were studied. As a computational example, a parabolic arc was selected. Variations of angle-of-attack, Mach number and thickness were considered. The aerodynamic solutions at base and calibration values of the flow parameter were computed by using the transonic code LTRAN2 developed by Ballhaus and Goorjian (Reference 14).

For a 6% parabolic arc at Mach number 0.8, the steady and unsteady aerodynamic pressure coefficients were computed at angle-of-attack 0.8° by strained coordinate perturbation method. This was based on the base and calibration angles-of-attack equal to 0.4° and 0.6° , respectively. The aerodynamic results obtained at angle-of-attack 0.8° by strained coordinate perturbation method were compared with those directly obtained by LTRAN2. The comparison is good.

For the 6% parabolic arc at zero angle-of-attack, the steady and unsteady aerodynamic results were computed at Mach number 0.86. This was based on the base and calibration Mach numbers equal to 0.854 and 0.856, respectively. Present results are compared with those directly obtained by LTRAN2. The comparison is good.

For a 6.5% thick parabolic arc at Mach number 0.85, aerodynamic pressure coefficients were computed by strained coordinate method. The base and calibration thicknesses were 6% and 7%, respectively. Present results compare well with those obtained directly by LTRAN2.

Finally, the use of the strained coordinate perturbation method in computing the transonic divergence dynamic pressure of a typical slender straight wing with conventional airfoil is illustrated. Since two-dimensional aerodynamics were used in obtaining the aerodynamic loads, the aeroelastic equations were derived by using strip theory. The solution for divergence dynamic pressure was obtained by Rayleigh's method (Reference 15).

As a computational example, a 10% thick parabolic arc airfoil section was selected. By using the aerodynamic force coefficients computed by the strained coordinate perturbation method, the effect of Mach number on transonic divergence dynamic pressure was studied. These results were compared with those obtained by linear subsonic aerodynamic theory.

Based on the present procedure a computer program to post process LTRAN2 aerodynamic data for strained coordinate perturbation method was written. The listing with user's manual is given. This program creates new steady state initial conditions for LTRAN2 by using the base and calibration steady state solutions obtained by LTRAN2 for varying the flow parameters.

SECTION II

STRAINED COORDINATE PERTURBATION EQUATIONS

In this section, the strained coordinate perturbation equations are presented. The equations are based on the assumptions that shocks are neither created nor destroyed during perturbation and the order of the perturbation is small. The main objective is to obtain from two or more solutions an algebraic relation that connects the flow variables for a range of one or more parameters, thus leading to a rapid computation of these related flows. The effect of shock movement during perturbation is accounted by using the procedure given in Reference 12.

Equations are presented for two-dimensional transonic inviscid flow governed by small-disturbance conditions.

The basic steady-state equation in a scaled form is given by

$$\phi_{xx} + \phi_{zz} = \phi_x \phi_{xx} \quad (1)$$

where (x, z) is a Cartesian Coordinate System, with x aligned with the airfoil chord and related to the physical coordinate system (\bar{x}, \bar{z}) by the transformation

$$x = \bar{x}, \quad z = \beta \bar{z} \quad (2)$$

where, if M_∞ is the freestream Mach number, then

$$\beta = 1.0 / (1 - M_\infty^2)^{1/2} \quad (3)$$

The potential $\phi(x, z)$ is expanded as a series in small parameter ϵ such as

$$\phi(x, z) = \phi_0(x', z) + \epsilon \phi_1(x', z) + \dots \quad (4)$$

where x' is the strained coordinate. Shock is assumed to be normal to the freestream, thus only x coordinate straining is required. Following the discussion given in Reference 12 the strained coordinate system is defined by

$$x = x' + \epsilon \delta x_s x_1(x') \quad (5)$$

where, if x'_s is the location of the shock in the (x', z) coordinates, then

$$x_1(x') = \frac{x' (1 - x'_s)}{x'_s (1 - x'_s)} \quad ; \quad 0 \leq x' \leq 1 \quad (6a)$$

$$x_1(x') = 0; \quad x' > 1, \quad x' < 0 \quad (6b)$$

and $\epsilon \delta x_s$ is the amount by which the shock moves during the perturbation.

If by some method, say finite difference, two solutions termed as base and calibration are known, then an expression for the disturbance velocity potential can be expressed as

$$\begin{aligned} \phi_x(x, z) = & \phi_{x'}^{(0)}(x', z) [1 - \epsilon \delta x_s x_{1x'}(x')] + \\ & \epsilon \phi_{1x'}(x', z) \dots \quad (7) \end{aligned}$$

where

$$\epsilon_0 \phi_{1x}(x', z) = \phi_{\hat{x}}^{(1)}(\hat{x}, z) - \phi_{x'}^{(0)}(x', z) [1 - \epsilon_0 \delta x_s x_{1x'}(x')]$$

$$\hat{x} = x' + \epsilon_0 \delta x_s x_1(x')$$

$$x = x' + \epsilon \delta x_s x_1(x')$$

$\epsilon_0 \delta x_s$ = the change in the shock location between base and calibration solutions

$\phi_{x'}^{(0)}$ = base solution

$\phi_{\hat{x}}^{(1)}$ = calibration solution

The expressions for the perturbations ϵ and ϵ_0 depend on the flow or geometry parameter perturbed. Following the discussion given in Reference 12 for Mach number variation the expressions for ϵ and ϵ_0 can be written as

$$\epsilon = \left[\frac{(\gamma+1)M_\infty^q}{(1-M_\infty^2)^{3/2}} - \frac{(\gamma+1)M_0^q}{(1-M_0^2)^{3/2}} \right] / \left[\frac{(\gamma+1)M_0^q}{(1-M_0^2)^{3/2}} \right] \quad (8a)$$

$$\epsilon_0 = \left[\frac{(\gamma+1)M_1^q}{(1-M_1^2)^{3/2}} - \frac{(\gamma+1)M_0^q}{(1-M_0^2)^{3/2}} \right] / \left[\frac{(\gamma+1)M_0^q}{(1-M_0^2)^{3/2}} \right] \quad (8b)$$

where γ = ratio of specific heats

M_0 = freestream Mach number of base flow

M_1 = freestream Mach number of calibration flow

M_∞ = current freestream Mach number

q = the exponent in the transonic parameter taken to be 2

For angle-of-attack variation the expressions for ϵ and ϵ_0 can be written

as

$$\epsilon = \alpha - \alpha_0 \quad (9a)$$

$$\epsilon_0 = \alpha_1 - \alpha_0 \quad (9b)$$

where

α = current angle-of-attack

α_1 = calibration angle-of-attack

α_0 = base angle-of-attack.

For thickness variation the expressions ϵ and ϵ_0 can be written as

$$\epsilon = \tau - \tau_0 \quad (10a)$$

$$\epsilon_0 = \tau_1 - \tau_0 \quad (10b)$$

where τ = current ratio of maximum thickness to chord of airfoil

τ_1 = ratio of maximum thickness to chord for calibration airfoil

τ_0 = ratio of maximum thickness to chord for base airfoil.

Based on the Equation 7 expressions for lift and moment coefficients can be written as

$$C_L = \frac{\beta^2}{k} \left\{ \left(\frac{k}{\beta^2} \right)^{(0)} C_{L_0} + \frac{\epsilon}{\epsilon_0} \left[\left(\frac{k}{\beta^2} \right)^{(1)} C_{L_1} - \left(\frac{k}{\beta^2} \right)^{(0)} C_{L_0} \right] \right\} \quad (11a)$$

$$C_m = \frac{\beta^2}{k} \left\{ \left(\frac{k}{\beta^2} \right)^{(0)} C_{m_0} + \frac{\epsilon}{\epsilon_0} \left[\left(\frac{k}{\beta^2} \right)^{(1)} C_{m_1} - \left(\frac{k}{\beta^2} \right)^{(0)} C_{m_0} \right] \right\} \quad (11b)$$

where C_L , C_{L_0} and C_{L_1} are lift coefficients corresponding to current, base and calibration values of the flow parameters, respectively; C_m , C_{m_0} and C_{m_1} are the moment coefficients corresponding to current, base and calibration values of the flow parameters, respectively; the transonic flow parameter k is defined as $(\gamma+1) M_\infty^2$, and (0) and (1) denote computations made at base and calibration values of the flow parameters, respectively.

SECTION III

APPLICATION TO STEADY AND UNSTEADY COMPUTATIONS

It is a common practice to conduct parametric studies in transonic aeroelasticity. Usually flow parameters such as Mach number and angle of attack are varied. In such cases the repetition of steady state computations can be avoided by using the strained coordinate perturbation method. Thus, there will be direct saving in the computational time for aeroelastic studies that depend on the steady state computations.

The unsteady computations based on time integration, indicial and harmonic methods depend on accurate steady state initial conditions. For given values of flow parameters, the steady state computation requires about 25 to 50 percent of computer time in transonic computer codes such as LTRAN2. Considerable amount of computer time can be saved by computing the steady state initial conditions from the strained coordinate perturbation method.

In this section, results are shown to illustrate the use of the strained coordinate perturbation method in steady and unsteady computations when Mach number, angle-of-attack and thickness ratio are varied. The airfoil considered is a parabolic arc. The Mach numbers considered were in the transonic range. The base and calibration solutions were obtained from LTRAN2 by using a finite difference mesh with 119 horizontal grid points and 79 vertical grid points.

a. Mach Number Variation

A parabolic airfoil of 6% maximum thickness-chord ratio at zero angle of attack was considered. Based on the base and calibration Mach numbers equal to 0.854 and 0.856, respectively, results for Mach number 0.86 was

obtained by strained coordinate perturbation method. They are compared with those obtained directly from LTRAN2.

Figure 1 shows the steady state pressure coefficient curve obtained by strained coordinate perturbation method for $M = 0.86$ by using Equation 7. The values for ϵ and ϵ_0 were obtained by Equations 8a and 8b as 0.0748 and 0.0240, respectively. The amount of shock movement $\epsilon_0 \delta x_s$ between the base and calibration Mach numbers was equal to 0.02 chord. The computational time required to obtain this curve was about 5 seconds on CYBER 74 computer.

In Figure 1, the steady state pressure curve obtained directly from LTRAN2 is also shown. The curve obtained by strained coordinate perturbation method agrees well with that obtained by LTRAN2. There are some discrepancies near the shock. They may be due to the lack of fine enough grid near the shock.

Based on the base and calibration steady state solutions obtained at Mach numbers 0.854 and 0.856, respectively, initial conditions for Mach number 0.86 were computed by the strained coordinate perturbation Equation 7. This was carried-out by using a computer program given in the Appendix. Using this steady state initial condition, unsteady results were computed by the time integration procedure of LTRAN2. The reduced frequency k_c was assumed as 0.1.

Figure 2 shows two sets of unsteady pressure curves obtained by using the present initial condition and the initial condition directly obtained by LTRAN2. The curves were obtained at non-dimensional time ωt equal to 18.06 radians, where ω is the circular frequency of oscillation.

In Figure 2, it can be observed that results obtained by the two methods agree well. Slight discrepancies in the initial steady state conditions obtained by the present method do not have any influence on the unsteady pressure

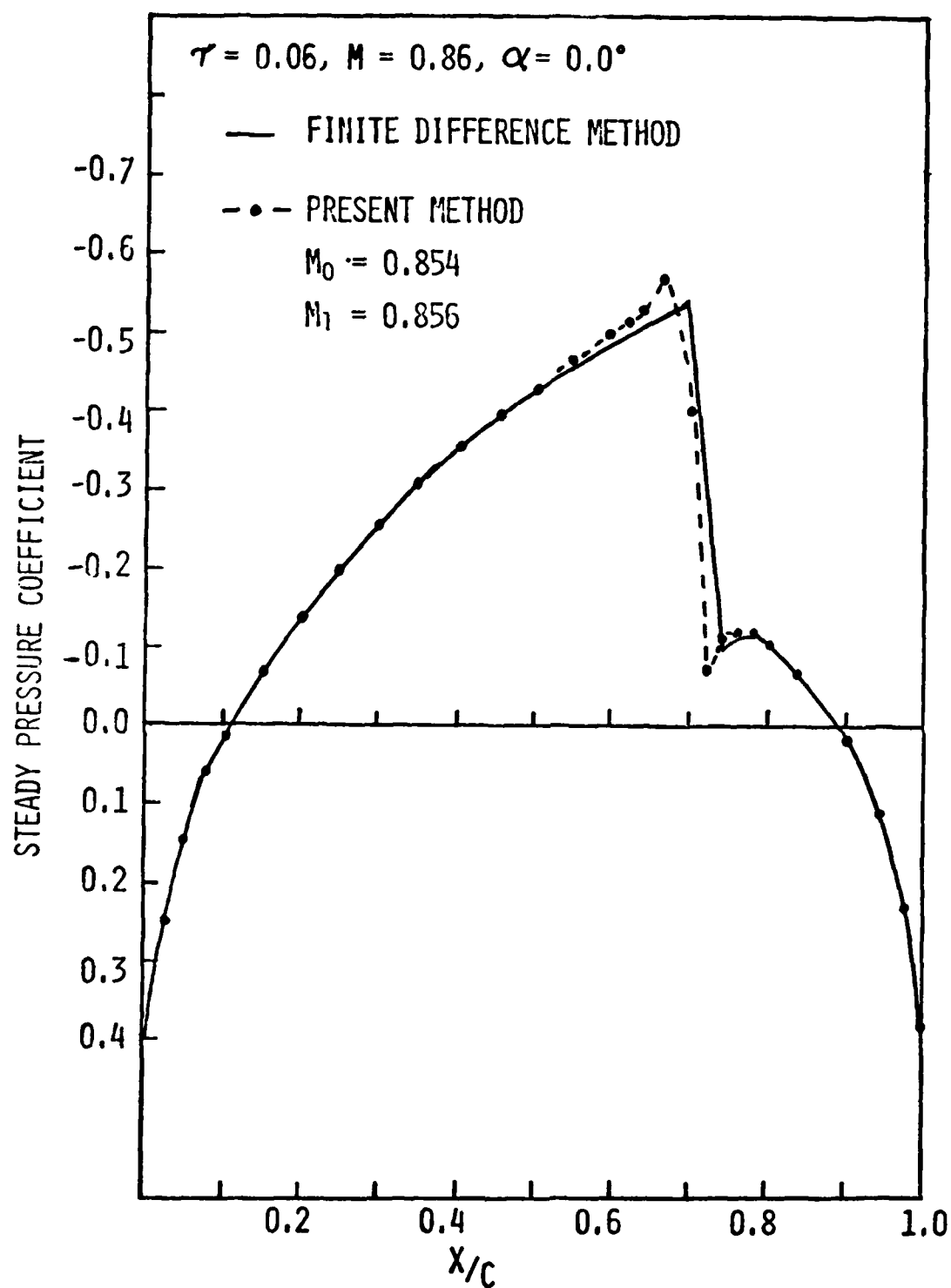


Figure 1. Effect of Mach Number Perturbation for 6% Thick Parabolic Arc on Steady Pressure Curves at $M = 0.86$.

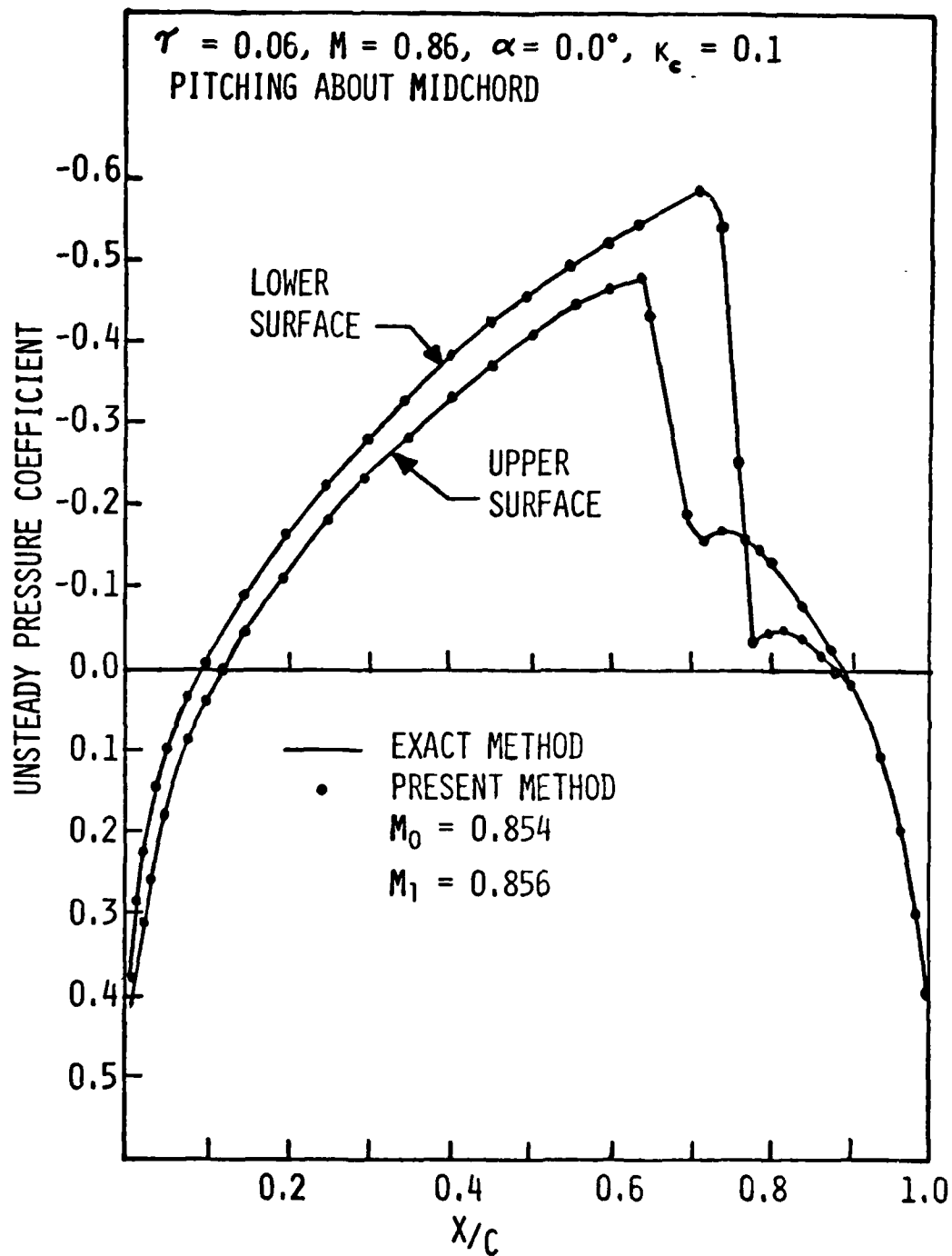


Figure 2. Effect of Mach Number Perturbation for 6% Thick Parabolic Arc on Unsteady Pressure Curves at $M = 0.86$.

curve. Similarly, unsteady lift and moment coefficients compared well between the two methods.

It was noticed that to obtain unsteady results for 3 cycles, the present method required about 60% of the computer time required for direct LTRAN2 computations. Based on the same base and calibration Mach numbers, steady and unsteady results can be obtained for Mach numbers, say, between 0.85 and 0.86. Thus, there can be a considerable saving in the computer time if additional aeroelastic computations have to be conducted in this range.

b. Angle-of-Attack Variation

The 6% thick parabolic arc at $M = 0.8$ was considered. Steady and unsteady aerodynamic results for angle-of-attack 0.8° was obtained by strained coordinate perturbation procedure. The base and calibration angles-of-attack were equal to 0.4° and 0.6° , respectively. Present results are compared with those directly obtained by LTRAN2.

The values for ϵ and ϵ_0 were obtained from Equations 9a and 9b as 0.4 and 0.2, respectively. Since there is no shock, the value for $\epsilon_0 \delta x_s$ is equal to zero.

Figure 3 shows the steady pressure curves obtained by both present procedure and LTRAN2. The agreement between the methods is excellent. The computational time required for the present procedure was about 5 seconds on the CYBER 74 computer.

Based on the base and calibration solutions, steady state initial conditions for unsteady computation was obtained by Equation 7 for angle-of-attack 0.8° . This was carried-out by using the computer program given in the Appendix. Using this initial condition, unsteady computations were conducted at reduced frequency $k_c = 0.1$ by pitching the airfoil at the midchord.

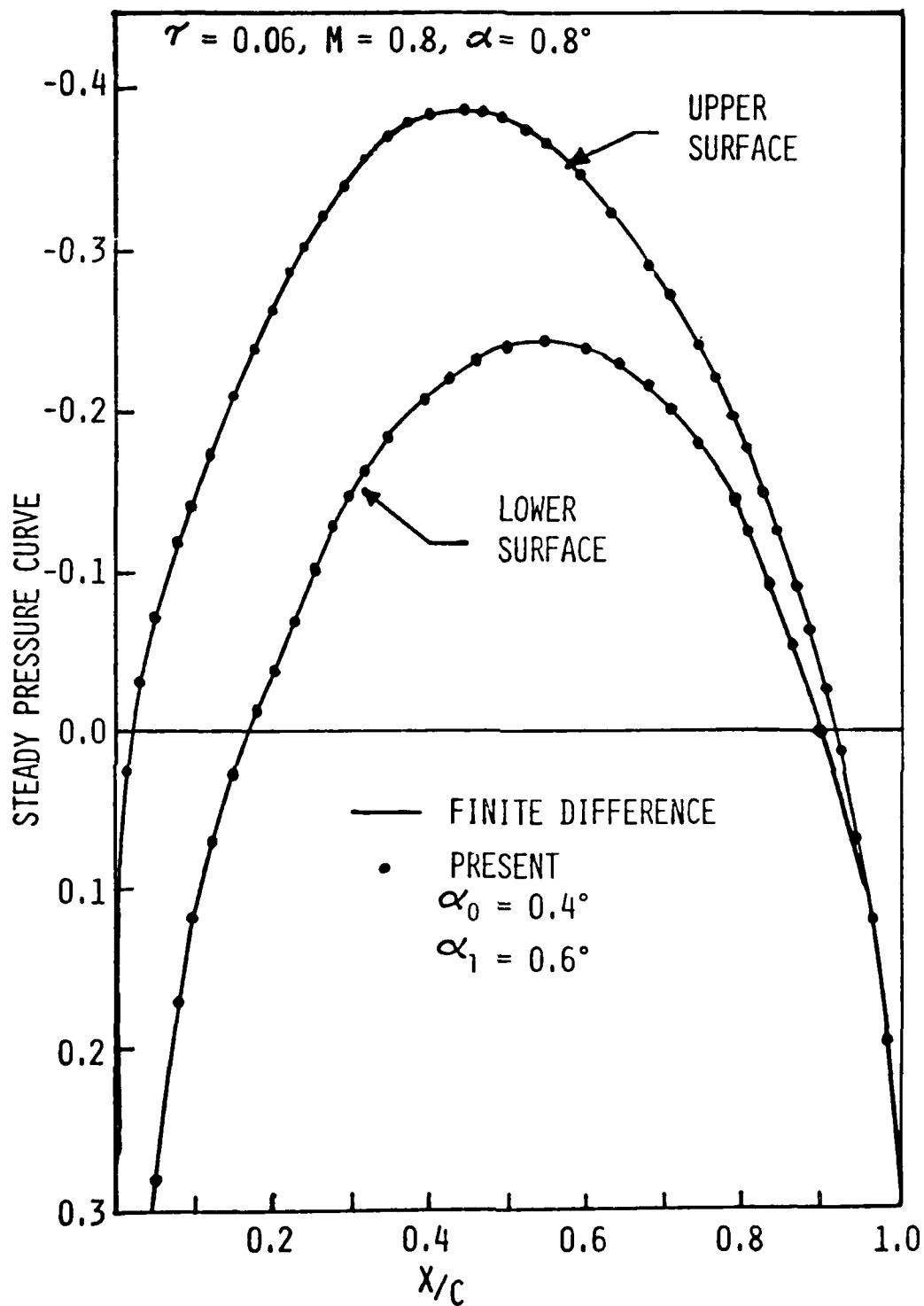


Figure 3. Effect of Angle of Attack Perturbation for 6% Thick Parabolic Arc on Steady Pressure Curves at $\alpha = 0.8^\circ$.

From unsteady computations it was found that the present method gives results identical to those obtained by LTRAN2 directly. This is because of the excellent comparison obtained between the two corresponding steady state curves.

It was noticed that to obtain unsteady results for 3 cycles, the present method required about 40% of the computer time required for direct LTRAN2 computations. Based on the same base and calibration angles-of-attack, steady and unsteady results can be obtained for angles-of-attack, say, between 0.0° and 1.0° from the present procedure. Thus, there can be considerable saving in the computer time if aeroelastic computations have to be conducted in this range.

c. Thickness Variation

A parabolic arc airfoil at Mach number 0.85 with zero angle-of-attack was considered. Based on base and calibration maximum thickness to chord ratios equal to 0.06 and 0.07, respectively, results for maximum thickness to chord ratio equal to 0.065 was obtained by strained coordinate perturbation method. They are compared with those obtained directly from LTRAN2.

Figure 4 shows the steady state pressure coefficient curve obtained by strained coordinate perturbation method for $\tau = 0.065$ by using Equation 7. The values for ϵ and ϵ_0 were obtained from Equations 10a and 10b as 0.005 and 0.01, respectively. The amount of shock movement $\epsilon_0 \delta x_s$ between the base and calibration thickness ratios was equal to 0.08 chord. The computational time required to obtain this curve was about 5 seconds on CYBER 74 computer.

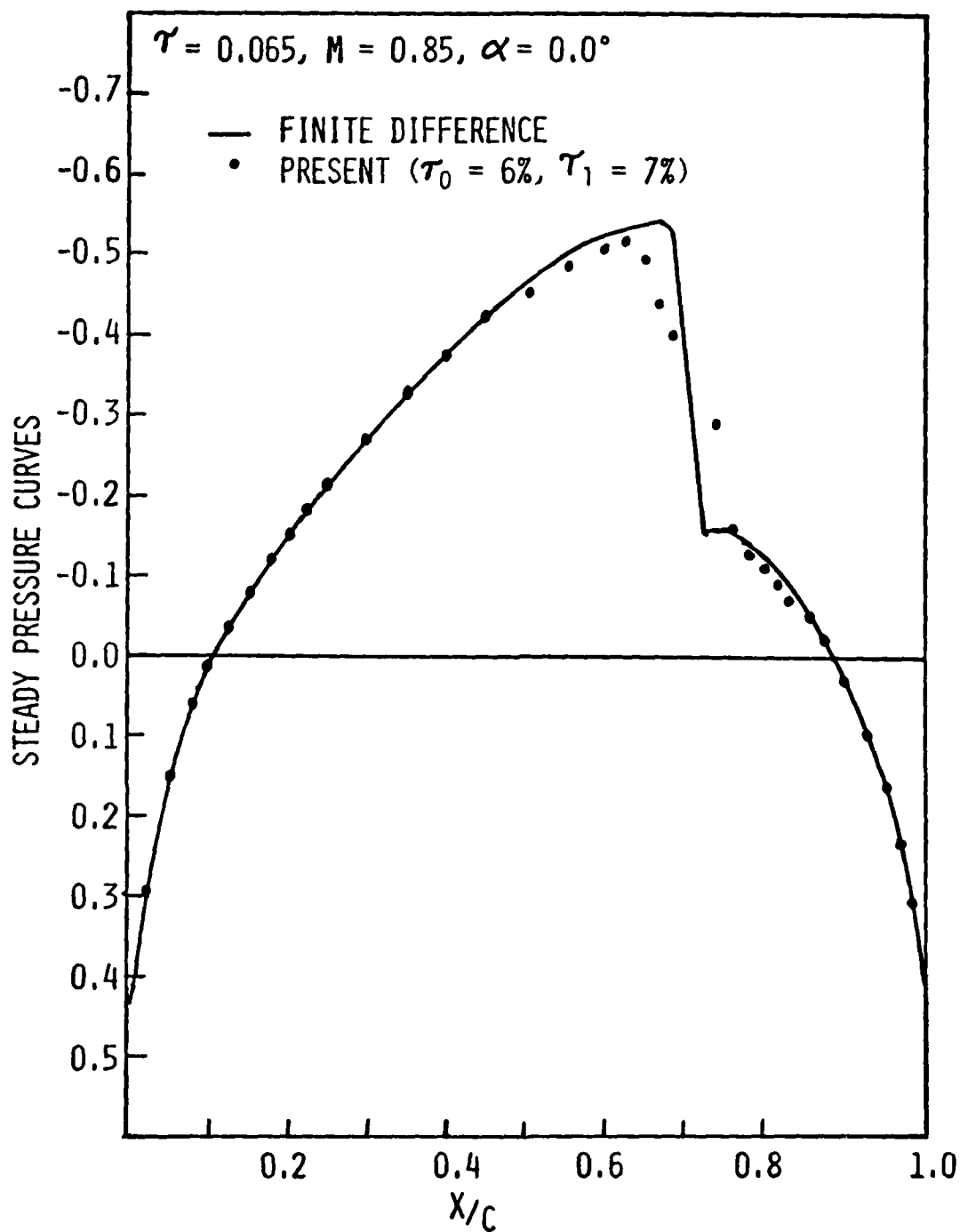


Figure 4. Effect of Thickness Perturbation for 6.5% Thick Parabolic Arc on Steady Pressure Curves at $M = 0.85$ and $\alpha = 0.0^\circ$.

In Figure 4, steady state pressure curve obtained directly from LTRAN2 is also shown. The agreement between two curves is good. There is some discrepancy near the shock. It may be due to lack of a fine grid near the shock.

Based on the base and calibration steady state solutions obtained at thickness ratios 0.06 and 0.07, respectively, initial conditions for thickness ratio equal to 0.065 was computed by the strained coordinate perturbation Equation 7. This was carried out by using a computer program given in the Appendix. Using this steady state initial condition, unsteady results were computed by time integration procedure of LTRAN2. The reduced frequency k_c was assumed as 0.1.

Figure 5 shows two sets of unsteady pressure curves obtained by using present initial conditions and initial conditions directly obtained by LTRAN2. The curves were plotted at non-dimensional time ωt equal to 18.06 radians.

In Figure 5, it can be observed that results obtained by the two methods agree well. Slight discrepancies in the initial steady state conditions obtained by present method do not have any influence on unsteady pressure curve. Similarly, the unsteady lift and moment coefficients compared well between the two methods.

It was noticed that to obtain unsteady results for 3 cycles, the present method required about 60% of the computer time required for the direct LTRAN2 computations. Based on the same base and calibration thickness ratios, steady and unsteady results can be obtained for thickness ratios, say, between 0.05 and 0.08 from present procedure. Thus, there can be considerable saving in the computer time if additional aeroelastic computations have to be conducted in this range.

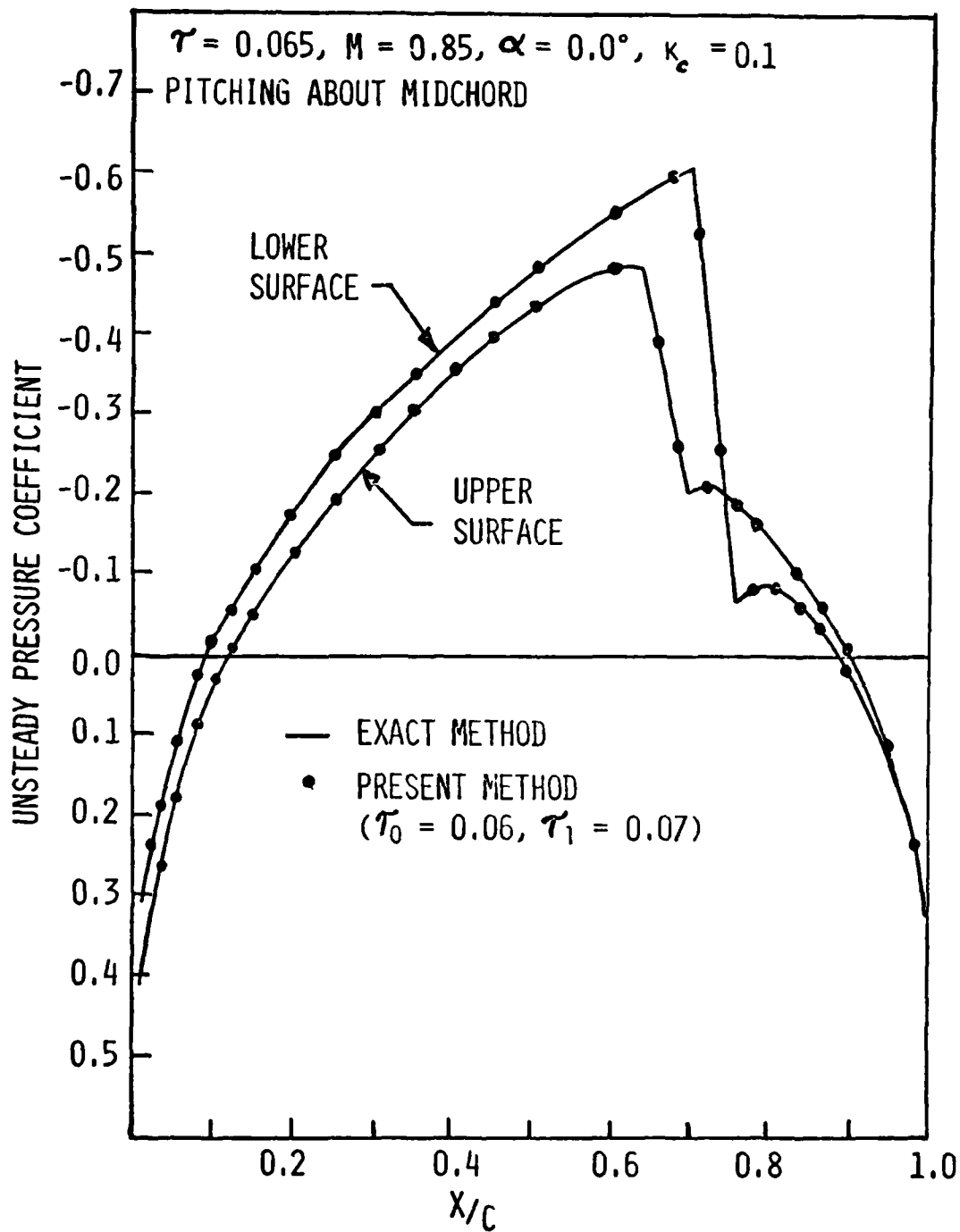


Figure 5. Effect of Thickness Perturbation for 6.5% Thick Parabolic Arc on Unsteady Pressure Curves at $M = 0.85$ and $\alpha = 0.0^\circ$.

SECTION IV

APPLICATION TO THE TRANSONIC DIVERGENCE PROBLEM

Based on the strained coordinate perturbation method, computational time required for transonic aeroelastic studies can considerably be reduced. One such study where this method can be used is in computing the transonic static divergence speeds of slender straight wings.

In this study, the transonic divergence dynamic pressure of a typical slender straight wing with conventional airfoil is computed by using the method of strained coordinates. The required base and calibration aerodynamic solutions were obtained by LTRAN2. Since two-dimensional aerodynamics was used in obtaining the aerodynamic loads, the aeroelastic equations were derived by using strip theory. The solution for divergence dynamic pressure was obtained by Rayleigh's method (Reference 15).

As a computational example, a 10% thick parabolic arc airfoil section was selected. First, the use of the method of strained coordinates was illustrated at a transonic Mach number of 0.8 for varying angle-of-attack. Then the effect of Mach number on transonic divergence dynamic pressure was studied for various positions of the elastic axis. These results were compared with those obtained by linear subsonic theory.

a. Formulation of Divergence Equations

It is assumed that the wing is slender and straight so that the three dimensional effects of the aerodynamics can be neglected and that strip theory can be used in deriving an expression for the static divergence dynamic pressure. Assuming that the wing torsional deformation pattern is invariable.

with respect to the load distribution and using Rayleigh's method an expression for the static divergence dynamic pressure can be written as

$$q_D = \frac{GJ \int_0^p \left(\frac{df}{d\xi} \right)^2 d\xi}{c^4 \int_0^p \{C_{\ell\alpha} (1 + a_h)/2 + C_{m\alpha}\} f^2 d\xi} \quad (12)$$

where $q_D = 1/2 \rho U^2$, is the divergence dynamic pressure; ρ , density of the air; U , flight speed; GJ , torsional rigidity of the wing section assumed to be constant along span; p , ratio of the span to chord; f , divergence mode shape expressed as a function of ξ ; ξ , is the ratio of the distance measured in full chords from the root to a span station; c , full chord length of the wing assumed to be constant along the span; $C_{\ell\alpha}$, slope of the aerodynamic lifting force with respect to the angle-of-attack; $C_{m\alpha}$, slope of the aerodynamic pitching moment (measured about the leading edge) with respect to the angle-of-attack; and a_h , position of the elastic axis measured in semi-chords from the midchord (positive towards trailing edge).

For the subsonic and supersonic flows the aerodynamic equations are linear and the aerodynamic force coefficients, C_ℓ and C_m , depend on the angle-of-attack linearly. Hence, Equation 12 can be integrated once an expression for $f(\xi)$ is assumed. On the other hand, for the transonic flows, the aerodynamic equations are non-linear and the aerodynamic force coefficients, C_ℓ and C_m , depend on angle-of-attack in a non-linear fashion. Hence, it is required to express C_ℓ and C_m as a function of angle-of-attack in order to integrate Equation 12. Such expression can be derived for transonic flows

by using the method of strained coordinates.

Assuming that perturbation in the angle-of-attack is small and the shock is neither created nor destroyed within the range of the perturbation, C_l and C_m can be expressed as (See Equations 11a and 11b)

$$C_l = C_{l_0} + (\epsilon/\epsilon_0) (C_{l_1} - C_{l_0}) \quad (13)$$

$$C_m = C_{m_0} + (\epsilon/\epsilon_0) (C_{m_1} - C_{m_0}) \quad (14)$$

where C_{l_1} and C_{l_0} are calibration and base lift coefficients, respectively; C_{m_1} and C_{m_0} are calibration and base moment coefficients (measured about the leading edge), respectively; $\epsilon = \alpha - \alpha_0$; $\epsilon_0 = \alpha_1 - \alpha_0$; α_1 is the calibration angle-of-attack; and α_0 is the base angle-of-attack.

Equations 13 and 14 lead to simple expression for C_{l_α} and C_{m_α} as

$$C_{l_\alpha} = (C_{l_1} - C_{l_0})/(\alpha_1 - \alpha_0) \quad (15)$$

$$C_{m_\alpha} = (C_{m_1} - C_{m_0})/(\alpha_1 - \alpha_0) \quad (16)$$

Since C_{l_α} and C_{m_α} given by Equations 15 and 16 are independent of α , Equation 12 can be integrated for a known function of $f(\xi)$. This function should approximately represent the divergent mode that satisfies the boundary conditions, namely, $f(0) = 0$ and $f'(p) = 0$. One such function is given by

$$f(\xi) = 2\xi/p - (\xi/p)^2 \quad (17)$$

Substituting Equations 15, 16 and 17, into 12 and integrating yields

$$\bar{q}_D = 15/6A \quad (18)$$

where $\bar{q}_D = q_D \rho^2 c^4/GJ$, non-dimensional static divergence dynamic pressure

$$\text{and } A = (C_{\ell_1} - C_{\ell_0}) (1 + a_h)/2(\alpha_1 - \alpha_0) + (C_{m_1} - C_{m_0})/(\alpha_1 - \alpha_0) \quad (19)$$

b. Results

The Mach numbers considered in this study are in transonic range for the 10% thick parabolic arc.

First, a case with angle-of-attack varying from 0° to 1.0° at Mach number 0.80 was considered to illustrate the use of the method of strained coordinates. Lift and moment coefficients were computed by both the finite difference and the strained coordinate methods and they are compared.

Figure 6 shows the plots of lift coefficient C_ℓ versus angle-of-attack obtained by both finite difference and strained coordinate methods. The curve for strained coordinate method was based on base and calibration angles-of-attack equal to 0.2° and 0.8° , respectively. The corresponding results for the pitching moment coefficient (about the leading edge) are shown in Figure 7. In both Figures 6 and 7, the aerodynamic computations at base and calibration angles-of-attack were also made by the successive line over relaxation method.

Results in Figures 6 and 7 show that the method of strained coordinates agree well with the finite difference method. The level of agreement is better for lift coefficients when compared to that for moment coefficients. The total computational time required by the method of strained coordinates was about 1/5 of that required for the finite difference method. Also the method of strained coordinates assumes simple relations between the aerodynamic force

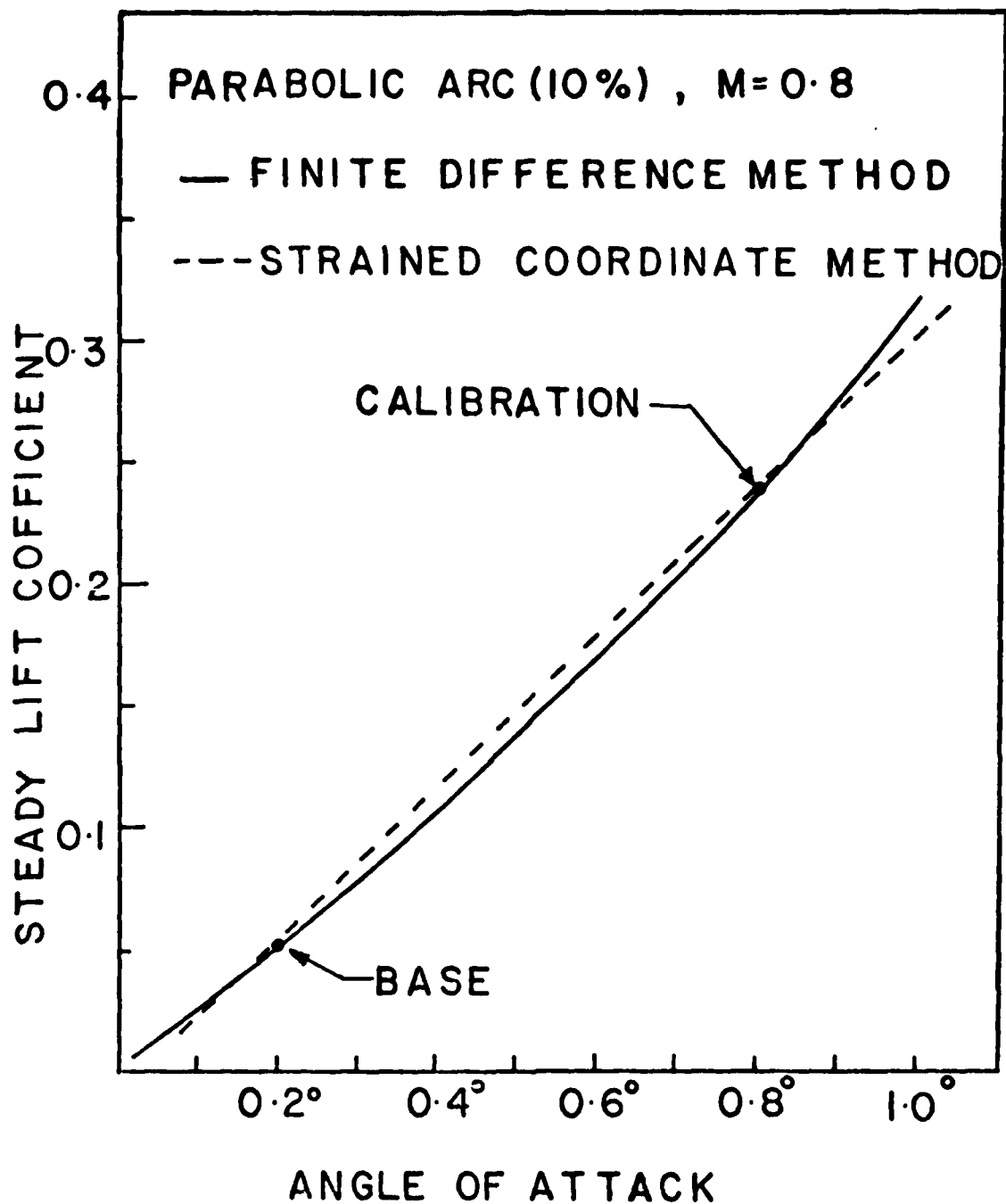


Figure 6. Variation of Lift Coefficient With Angle of Attack for 10% Thick Parabolic Arc at $M = 0.80$.

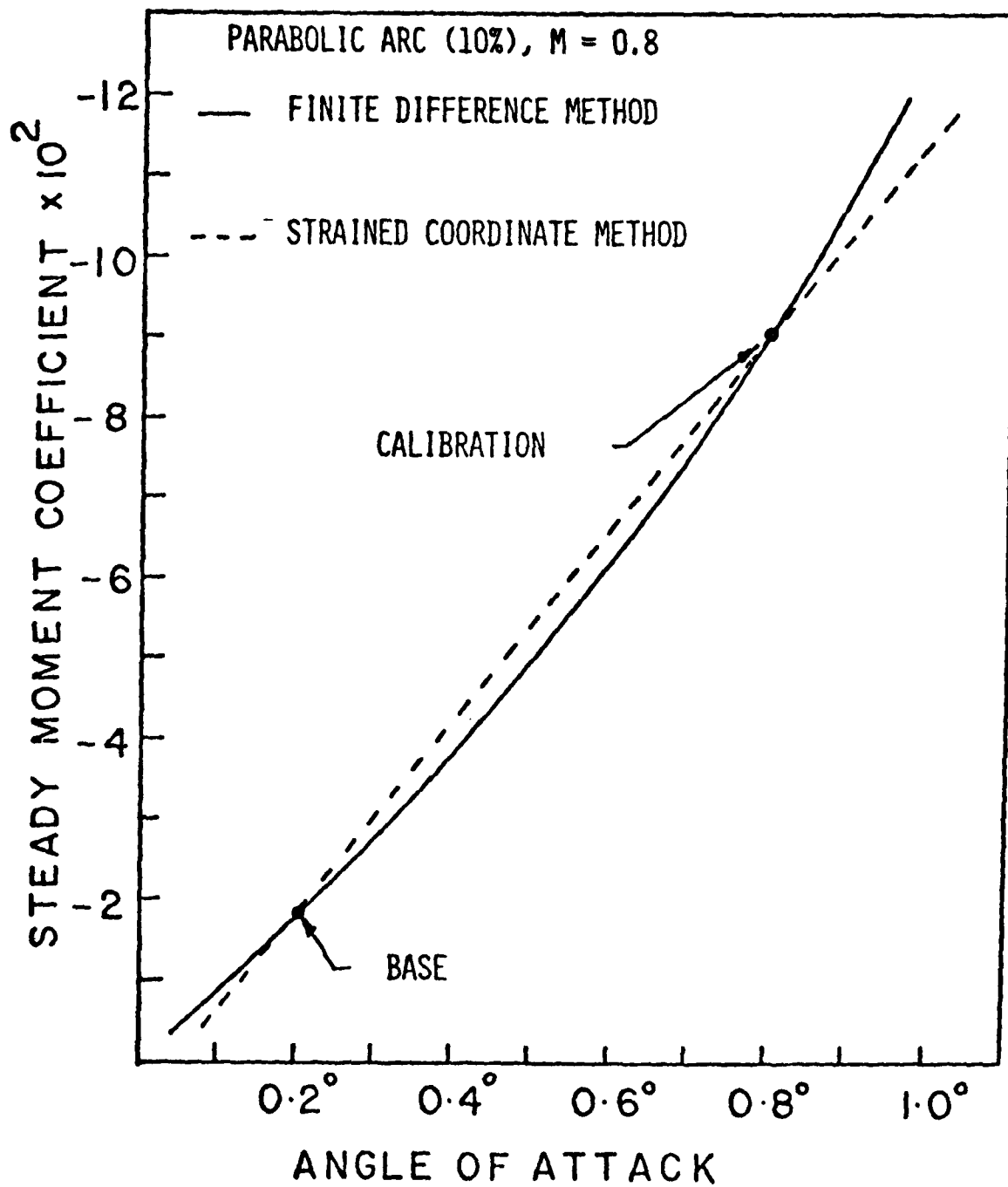


Figure 7. Variation of Moment (About Leading Edge) Coefficient With Angle of Attack for 10% Thick Parabolic Arc at $M = 0.80$.

coefficients and the angle-of-attack.

The application of the method of strained coordinates in computing the transonic divergence characteristics was considered next. The characteristics of the static divergence dynamic pressures for varying Mach number at various values of the position of elastic axis were obtained. The base and the calibration angles were assumed as 0.2° and 0.6° , respectively. The Mach numbers considered were 0.76, 0.78, 0.79, 0.80, 0.805, and 0.81, respectively.

Table 1 shows the lifting force and pitching moment (about the leading edge) coefficients obtained at base and calibration angles-of-attack for six Mach numbers. It is observed in the table that both the coefficients increase non-linearly with increase in Mach number. In the same table corresponding coefficients obtained by linear aerodynamic theory are also given for reference. The differences in the values are mainly due to the presence of shocks.

Based on the aerodynamic coefficients given in Table 1 and using Equation 18, static divergence dynamic pressures were computed. The values for the position of elastic axis were assumed as 0.0, -0.1, and -0.2. Figure 8 shows the plots of divergence dynamic pressure parameter \bar{q}_D versus Mach number. In the same figure the corresponding results obtained by the subsonic theory are also shown.

In Figure 8, it is observed that the static divergence dynamic pressure obtained by transonic aerodynamics increased with the increase of Mach number. The increase is more rapid at higher Mach numbers. Also the static divergence dynamic pressure increases as the elastic axis move towards leading edge from the midchord. The curves shift to the left as the elastic axis moves toward the leading edge from the midchord.

TABLE 1 AERODYNAMIC COEFFICIENTS FOR 10% THICK
PARABOLIC ARC AT VARIOUS MACH NUMBERS

MACH NUMBER	CASE	Lift Coef. C_L		Moment Coef. C_m	
		$\alpha = 0.2^\circ$	$\alpha = 0.6^\circ$	$\alpha = 0.2^\circ$	$\alpha = 0.6^\circ$
0.760	1	0.03893	0.11710	-.01139	-.03426
	2	0.01074	0.03222	-.00268	-.00806
0.780	1	0.04308	0.13033	-.01314	-.03994
	2	0.01116	0.03347	-.00280	-.00837
0.790	1	0.04699	0.14380	-.01503	-.04681
	2	0.01139	0.03416	-.00285	-.00854
0.800	1	0.05477	0.17158	-.01945	-.06275
	2	0.01164	0.03491	-.00291	-.00873
0.805	1	0.06222	0.19965	-.02382	-.07989
	2	0.01177	0.03530	-.00294	-.00882
0.810	1	0.07322	0.25171	-.03050	-.11251
	2	0.01190	0.0357	-.00298	-.00893

1. Transonic Method

2. Subsonic Method

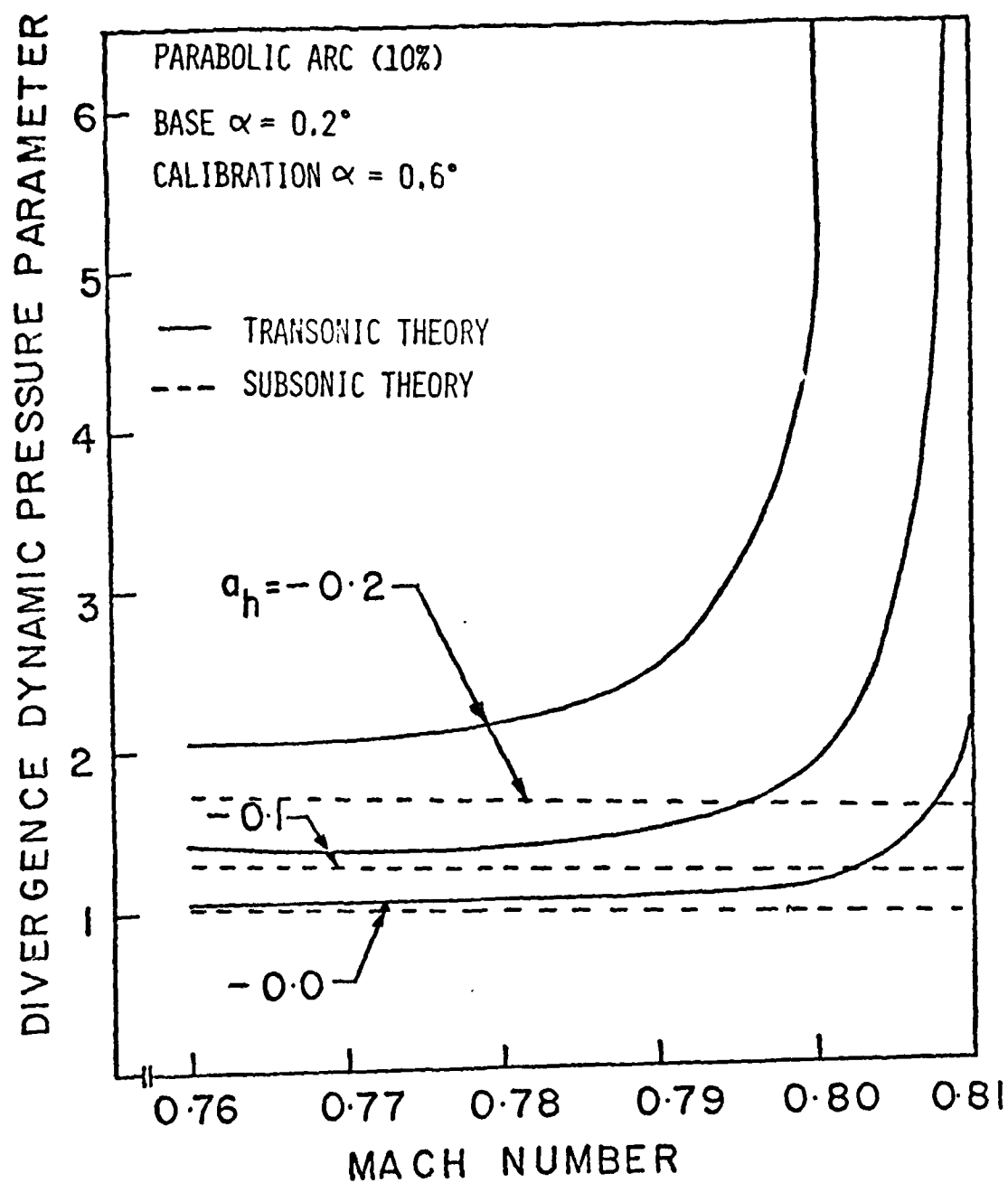


Figure 8. Effect of Mach Number on Static Divergence Dynamic Pressure for a Straight Slender Wing at Various Positions of Elastic Axis.

Figure 8 shows that the results obtained by subsonic theory do not agree with those obtained by the present transonic theory, especially at higher Mach numbers. Also agreement becomes bad as the elastic axis moves towards the leading edge. The discrepancies are mainly due to the presence of shocks which are incorporated only in the transonic theory. It is noted that the rapid changes in the divergence dynamic pressures at the higher Mach numbers are due to the movement of the shock towards the trailing edge.

The increase in the divergence dynamic pressures with the increase of Mach number can further be explained as follows. The center of pressure (CP) moves from the quarter chord towards midchord with increasing Mach number. Thus CP moves towards the elastic axis which is located near mid-chord for this study. As a result, the divergence dynamic pressure increases (See Equation 8-40 of Reference 15).

SECTION V

CONCLUDING REMARKS

Based on the present study the following concluding remarks may be made.

- (1) The steady state pressure curves obtained by using strained coordinate perturbation method compare well with those directly obtained by LTRAN2. Some small discrepancies obtained near the shock are due to the lack of a fine enough grid.
- (2) The computational time required to compute the steady state pressure curve by the strained coordinate perturbation method for a known base and calibration solution is about 5 seconds on CYBER 74 computer.
- (3) Unsteady results based on the initial conditions obtained by the present method compare well with those obtained directly by LTRAN2.
- (4) The present procedure shows about 40 to 50% saving in the computer time for typical unsteady computations required in aeroelastic analysis.
- (5) Based on aerodynamic forces computed by the strained coordinate perturbation equations, transonic divergence speeds of slender straight wings can be computed.
- (6) Based on the present computations it is found that the divergence speed of a slender straight wing with 10% thick parabolic arc section increase with increase in Mach number. On the other hand, linear theory predicts a different behavior.
- (7) The present procedure can be extended to three dimensional steady and unsteady transonic computations by using the corresponding developments in strained coordinate methods.

REFERENCES

1. Yang, T.Y., Striz, A.G., and Guruswamy, P., "Flutter Analysis of Two-Dimensional and Two Degree of Freedom Airfoils in Small Disturbance Unsteady Transonic Flow", AFFDL-TR-78-202, December 1978.
2. Yang, T.Y., Guruswamy, P., and Striz, A.G., "Aeroelastic Response Analysis of Two-Dimensional Single and Two-Degree-of-Freedom Airfoils in Low Frequency, Small Disturbance Unsteady Transonic Flow", AFFDL-TR-79-3077, June 1979.
3. Yang, T.Y., Guruswamy, P., Striz, A.G., and Olsen, J.J., "Flutter Analysis of a NACA 64A006 Airfoil in Small Disturbance Transonic Flow", *Journal of Aircraft*, Vol. 17, No. 4, April 1980.
4. Yang, T.Y., Guruswamy, P., and Striz, A.G., "Flutter Analysis of a Two-Dimensional and Two-Degree-of-Freedom Supercritical Airfoil in Small Disturbance Unsteady Transonic Flow", AFWAL-TR-80-3010, March 1980.
5. Yang, T.Y., Striz, A.G., and Guruswamy, P., "Flutter Analysis of a Two-Dimensional and Two-Degree-of-Freedom MBB A-3 Supercritical Airfoil in Two-Dimensional Transonic Flow", AIAA Paper No. 80-0736, May 1980.
6. Eastep, F.E., and Olsen, J.J., "Transonic Flutter Analysis of a Rectangular Wing with Conventional Airfoil Section", AIAA Paper No. 79-1632, August 1979.
7. Ashley, H., "On the Role of Shocks in the Sub-Transonic Flutter Phenomenon", AIAA Paper 79-0765, April 1979.
8. Lighthill, M.J., "A Technique for Rendering Approximate Solutions to Physical Problems Uniformly valid", *Philos. Mag.*, Vol. 40, 1949, pp. 1179-1201.
9. Van Dyke, M. Perturbation Methods in Fluid Mechanics, The Parabolic Press, California, 1975.
10. Stahara, S.S., Crisalli, A.J., and Spreiter, J.R., "Evaluation of a Strained Coordinate Perturbation Procedure: Nonlinear Subsonic and Transonic Flows", AIAA Paper 80-0339, January, 1980.
11. Nixon, D., "Perturbation of a Discontinuous Transonic Flow", AIAA Journal, Vol. 16, January 1978, pp. 47-52.

12. Nixon, D., "Perturbations in Two- and Three-Dimensional Transonic Flows", AIAA Journal, Vol. 16, July 1978, pp. 699-709.
13. Nixon, D., "Observations on the Strained Coordinate Method for Transonic Flows", AIAA Journal, Vol. 18, March 1980, pp. 341-342.
14. Ballhaus, W.F., and Goorjian, P.M., "Implicit Finite Difference Computations of Unsteady Transonic Flows About Airfoils", AIAA Journal, Vol. 15, December 1977, pp. 1728-1735.
15. Bisplinghoff, R.L., Ashley, H., and Halfman, R.L., Aeroelasticity, Addison Wesley Publishing Company, Reading Mass., 1955, Chapter 8.

APPENDIX

A computer program to create the steady state initial conditions by using the strained coordinate perturbation method is presented. This program is compatible for LTRAN2. This program can create a new steady state initial condition based on base and calibration steady state initial conditions obtained by LTRAN2.

a. Description of the INPUT

(1) Initial DATA Card (4I5, 4F10.4) one card to define following parameters.

<u>Columns</u>	<u>Description</u>	<u>Variable</u>
1-5	Number of mesh points in vertical direction	LMAX
6-10	Number of mesh points in horizontal direction	JMAX
11-15	Mesh point corresponding to leading edge	JLE
16-20	Mesh point corresponding to trailing edge	JTE
21-30	Distance of the shock from leading edge measured in chords for base flow	XS0
31-40	Distance of the shock from leading edge measured in chords for calibration flow	XS1
41-50	Value of the perturbation parameter ϵ (See Section II)	EP
51-60	Value of the perturbation parameter ϵ_0 (See Section II)	EPO

(2) Mesh Card (8E10.4)

Cards to define JMAX values of the X mesh points.

(b) Description of Logical Files Used

- TAPE 1 Contains steady state initial conditions from LTRAN2 for
 base flow on INPUT
- TAPE 2 Contains steady state initial conditions from LTRAN2 for
 calibration flow on INPUT
- TAPE 3 Contains the steady state initial conditions to LTRAN2
 for the current flow on OUTPUT

```

PROGRAM MAIN(INPUT,OUTPUT,TAPE5=INPUT,TAPE6=OUTPUT,TAPE1,
1 TAPE2,TAPE3,TAPE4)
DIMENSION PU(119),PL(119),P(79,119),DUMY1(119),DUMY2(119),
1 X(119),TX(119)

C
C PROGRAM TO CREATE STEADY STATE INTIAL CONDITIONS FOR LTRAN2
C BY STRAINED COORDINATE PERTURBATION METHOD
C JMAX=NUMBER OF HORIZONTAL GRID POINTS USED LTRAN2
C LMAX=NUMBER OF VERTICAL GRID POINTS USED IN LTRAN2
C JLE=HORIZONTAL GRID POINT OF LEADING EDGE
C JTE=HORIZONTAL GRID POINT OF TRAILING EDGE
C XSO=SHOCK POSITION IN BASE SOLUTION
C XS1=SHOCK POSITION IN CALIBRATION SOLUTION
C EP=VALUE OF PERTURBATION PARAMETER FOR CURRENT FLOW
C EPO=VALUE OF PERTURBATION PARAMETER FOR CALIBRATION FLOW
C X=X COORDINATES OF HORIZONTAL GRID POINTS
C NOTE - TAPE1 SHOULD CONTAIN STEADY STATE INTIAL CONDITIONS
C OF BASE FLOW FROM LTRAN2
C TAPE2 SHOULD CONTAIN STEADY STATE INTIAL CONDITIONS
C OF CALIBRATION FLOW FROM LTRAN2
C ON OUTPUT TAPE3 WILL CONTAIN STEADY STATE INTIAL CONDITIONS
C OF THE CURRENT FLOW FOR LTRAN2
C INTIAL CONDITIONS FROM LTRAN2 ARE
C T=TIME
C GLIFT=LIFT
C PU=DISTURBANCE VELOCITY POTENTIALS OF UPPER SURFACE
C PL=DISTURBANCE VELOCITY POTENTIALS OF LOWER SURFACE
C P=DISTURBANCE VELOCITY POTENTIALS OF ALL GRID POINTS
C

READ(5,1)LMAX,JMAX,JLE,JTE,XSO,XS1,EP,EPO
1 FORMAT(4I5,6F10.4)
DXS=XS1-XSO
WRITE(6,6)LMAX,JMAX,JLE,JTE,XSO,XS1,DXS,EP,EPO
6 FORMAT(/5X,*NO OF VER MESH POINTS=*,I5,* NO OF HOR MESH PTS=*,I5,
1 * LE MESH PT=*,I5,*TE MESH PT=*,I5 , /5X,*BASE SHOCK POSITION=*,
2,F10.4,*CAL SHOCK POSITION=*,F10.4,* SHOCK DISPLACEMENT=*,F10.4/5X,
3, * EP=*,F10.4,* EPO=*,F10.4)
READ(6,7)(X(I),I=1,JMAX)
7 FORMAT(8E10.4)
WRITE(6,11)
11 FORMAT(/5X,* X CO-ORDINATES*)
WRITE(6,18)(X(I),I=1,JMAX)
18 FORMAT(/5X,10F12.6)
CONS=XSO*(1.0-XSO)
DO 20 I=1,JMAX
20 TX(I)=0.0
DO 30 I=JLE,JTE
30 TX(I)=(X(I)*(1.0-X(I)))/CONS
WRITE(6,31)
31 FORMAT(/5X,*DISTORSION COEF=*)
WRITE(6,36)(TX(I),I=1,JMAX)
36 FORMAT(/5X,10F12.6)
REWIND 1
READ(1)T1,LMAX1,JMAX1,GLIFT1, (PU(J),PL(J),(P(L,J),L=1,LMAX),
1 J=1,JMAX)
WRITE(6,2)
2 FORMAT(/5X,* DATA FROM TAPE1*)
WRITE(6,41)T1,LMAX1,JMAX1,GLIFT1
41 FORMAT(/5X,F10.4,2I5,F10.4)
DO 10 I=1,JMAX
WRITE(6,16) I,PU(I),PL(I)
16 FORMAT(/5X,*FOR COLUMN=*,I5,*PU=*,E15.6,* PL=*,E15.6)
WRITE(6,17)(P(J,I),J=1,10)
17 FORMAT(/5X,10E12.4)
10 CONTINUE
REWIND 3
WRITE(3)(PU(I),I=1,JMAX)
WRITE(3)(PL(I),I=1,JMAX)
DO 40 I=1,LMAX
40 WRITE(3)(P(I,J),J=1,JMAX)

```

```

REWIND 2
READ(2)T2,LMAX2,JMAX2,GLIFT2, (PU(J),PL(J),(P(L,J),L=1,LMAX),
1 J=1,JMAX)
WRITE(6,21)
21 FORMAT(/5X,* DATA FROM TAPE 2*)
WRITE(6,41)T2,LMAX2,JMAX2,GLIFT2
DO 100 I=1,JMAX
WRITE(6,16)I,PU(I),PL(I)
100 WRITE(6,17)(P(J,I),J=1,10)
RA=EP/EPO
REWIND 4
REWIND 3
C1=RA*DXS
READ(3)(DUMY1(I),I=1,JMAX)
DO 200 I=1,JMAX
200 DUMY2(I)=DUMY1(I)*(1.0-C1*TX(I))+RA*(PU(I)-DUMY1(I)*
1(1.0-DXS*TX(I)))
WRITE(4)(DUMY2(I),I=1,JMAX)
READ(3)(DUMY1(I),I=1,JMAX)
DO 300 I=1,JMAX
300 DUMY2(I)=DUMY1(I)*(1.0-C1*TX(I))+RA*(PL(I)-DUMY1(I)*
1(1.0-DXS*TX(I)))
WRITE(4)(DUMY2(I),I=1,JMAX)
DO 500 I=1,LMAX
READ(3)(DUMY1(K),K=1,JMAX)
DO 400 J=1,JMAX
400 DUMY2(J)=DUMY1(J)*(1.0-C1*TX(J))+RA*(P(I,J)-DUMY1(J)*
1(1.0-DXS*TX(J)))
500 WRITE(4)(DUMY2(K),K=1,JMAX)
T3=T1+RA*(T2-T1)
GLIFT3=GLIFT1+RA*(GLIFT2-GLIFT1)
REWIND 4
REWIND 3
READ(4)(PU(I),I=1,JMAX)
READ(4)(PL(I),I=1,JMAX)
DO 600 I=1,LMAX
600 READ(4)(P(I,J),J=1,JMAX)
WRITE(3)T3,LMAX1,JMAX1,GLIFT3, (PU(J),PL(J),(P(L,J),L=1,LMAX),
1 J=1,JMAX)
REWIND 3
READ(3)T3,LMAX1,JMAX1,GLIFT3, (PU(J),PL(J),(P(L,J),L=1,LMAX),
1 J=1,JMAX)
WRITE(6,601)
601 FORMAT(/5X,* DATA TO BE WRITTEN ON TAPE 3*)
WRITE(6,41)T3,LMAX1,JMAX1,GLIFT3
DO 700 I=1,JMAX
WRITE(6,16)I,PU(I),PL(I)
700 WRITE(6,17)(P(J,I),J=1,10)
STOP
END

```

**DA
FILM**

EN

DAT
FILME

2

DTIC